BOBCAT - a photon-efficient multi-way combiner for the VLTI

David Buscher, Fabien Baron, Julien Coyne, Chris Haniff, John Young

Astrophysics Group, Cavendish Laboratory, University of Cambridge, UK

Summary. We describe a concept for a near-infrared (JHK) bulk-optics combiner designed for efficient model-independent imaging of faint sources. The combiner is designed to accommodate (through a reconfigurable switchyard) any number of input beams from three to six. The instrument will include its own group-delay fringe tracker in addition to the "science" beam combiner. This will mean that fringe tracking will be possible using baseline "bootstrapping" while science data can be being secured on much longer baselines where the fringe visibility may be very low. We expect that a photon-efficient optical design will allow faint ($K \sim 13$) science targets to be observed, including AGN. Our proposed instrument will allow the full imaging potential of the VLTI infrastructure to be realised.

1 Science case

The scientific productivity of VLTI would be greatly enhanced if model-independent images could be made routinely. For all science programmes the existing VLTI capability of measuring visibilities and closure phases on a small number of baselines/triangles suffices when one is sure a source can be correctly represented by one of a small number of competing models, each with only a few unknown parameters. However, for many astrophysical problems the situation is more complex — models may have many parameters, the number of competing models may be large, or no available model may fit the interferometric data. Under these circumstances it can become possible to draw completely erroneous conclusions if an incorrect model is used. The ability to reconstruct model-independet images is the key to allowing reliable scientific conclusions to be drawn.

The first-generation VLTI instruments (particularly AMBER) do in principle allow the reconstruction of model-independent images, but this would require multiple reconfigurations of the ATs and/or the VLTI beam relay optics. Hence it is often difficult for potential observers to justify the amount of telescope time needed for imaging. Even if time is awarded, only a small fraction of the visibility phase information is likely to be measured, leading to lower-quality images for the same (u, v)-plane coverage compared with an instrument that can interfere more beams simultaneously.

We propose here a beam combiner designed to make effective use of the beams from up to six telescopes simultaneously, and thereby make rapid

imaging with the VLTI a reality. The instrument makes use of a proven bulk-optics combiner design together with a dedicated fringe tracker, and has the name "Bulk Optics Beam Combiner And Tracker" or BOBCAT.

Space does not permit the elaboration of the full science reference mission for an imaging interferometric instrument, which is detailed in our report for the EU JRA4 "WP 1.1 Advanced Instruments Initial Matrix Document", dated March 24th 2005. Our reference misson concentrates on four main fields of research, young stellar objects (YSOs), the study of stellar multiplicity, the late stages of stellar evolution (dust shells), and active galactic nuclei. In all cases, we concentrate on the science that can be offered by *imaging* of moderately complex objects as opposed to measurement of model parameters of simple (i.e. few-parameter) models. A notable feature of this mission is that it is very broad, in that it covers a large range of astrophysical research, and is therefore likely to appeal to a wide range of ESO astronomers.

2 Derived top-level requirements for imaging

Given a science case which rests on the imaging of complex sources, we can ask how this top-level science requirement flows down to top-level requirements on the implementation. The major requirements can be summarised as (a) adequate (u, v)-plane coverage (b) adequate phase information, and (c) a real-time fringe-tracking system which is appropriate for resolved sources. We discuss each of these requirements briefly below.

The relationship between (u, v)-plane coverage and image quality is a topic which has been well covered in studies of radio synthesis imaging, and these are equally applicable to the optical/IR domain. "Rules of thumb" have been developed which capture the overall requirements for a given imaging scenario. The most important of these is that if one is intending to make an image with a given number N of "filled pixels" (this is a rough measure of how many resolution-element-sized regions in the image are emitting significant flux) then one needs to have visibility amplitude and phase measurements for least N *independent* points in the (u, v) plane. "Independent" points are those which are at least λ/θ apart in the Fourier plane, where λ is the mean wavelength of observation and θ is a measure of the overall angular extent of the object.

Thus in order to make a 10×10 pixel image with an angular resolution of θ_0, one would need to make approximately 100 visibility measurements, spaced at intervals of about $\lambda/(10\theta_0)$ and spread over a region of radius λ/θ_0 in the (u, v) plane. With only 3 telescopes, we sample only 3 points in the (u, v) plane at any one time. Earth rotation synthesis will allow more data points to be collected over time, but the number of *independent* data points will not be large: typically the maximum image complexity that could potentially be reconstructed even after eight hours of rotation synthesis with an ideally-spaced array of 3 telescopes would be about 3×3 resolution elements.

Thus in order to make images of even modest complexity, either repeated relocation of the telescopes or combining the beams from more telescopes is required. The latter is likely to be a much more efficient use of telescope time: increasing the number of telescopes combined from 3 to 4 increases the number of (u, v) points sampled by a factor of 2, and going to six beams increases the (u, v) sampling by another factor of 2.5, i.e. a 6-telescope array would be 5 times faster than a 3-telescope array in covering the (u, v) plane.

It is commonly recognised that in order to reconstruct images from interferometers, measurements of visibility phase information are required: measurements of visibility amplitudes alone are not usually sufficient to reliably make images. Experience from radio astronomy over the last 50 years has shown that the two main techniques for recovering phase information in the presence of phase perturbations (as are present in all ground-based optical/IR interferometric measurements) are closure phase and phase-referencing. Closure phases require the simultaneous measurement of fringes on three or more baselines, whereas phase referencing relies on simultaneous measurements of phases on the science target and a nearby unresolved reference source. In the optical/IR regime, measurement of closure phases to accuracies of fractions of a degree requires quite simple hardware, whereas phase referencing at the same level, e.g. with the PRIMA instrument, requires a number of complex, precise and expensive subsystems in order to work. Typically therefore, phase referencing can be applied on only a few baselines at a time, thereby restricting the available (u, v) coverage. Nevertheless, phase referencing is thought by some astronomers to be preferable to using closure phases, because they have concerns related to the well-known result that (except in a limited range of circumstances) there is no unique way of deriving a set of object phases from a set of closure phases.

We can use simulations to get an idea of the relative importance of the various forms of phase information and (u, v) coverage to the quality of the images that can be reconstructed. Figure 1 shows the results from simulations of imaging with high signal-to-noise data (SNR>100:1 per visibility data point) as a function of two variables: the (u, v) coverage and the source of the phase information. Interferometric data were generated simulating 6-hour Earth-rotation synthesis observations of a test source (an extended eliptical star with a binary companion). Data were generated corresponding to using arrays of either 4 or 6 telescopes. For each array, either phase-referenced data (in the simulations, simply the object phases with $\sim$0.01 radians of added noise) or closure phase data (with identical amounts of noise) were generated, giving a total of 4 datasets. Each of these datasets were used for image reconstruction and the results are shown in Figure 1.

It is readily apparent from the figure that the difference in resulting image quality between using 4 and using 6 telescopes is much greater than that between using the phases resulting from phase referencing and closure phases. This confirms that the closure phase captures a large fraction of the phase

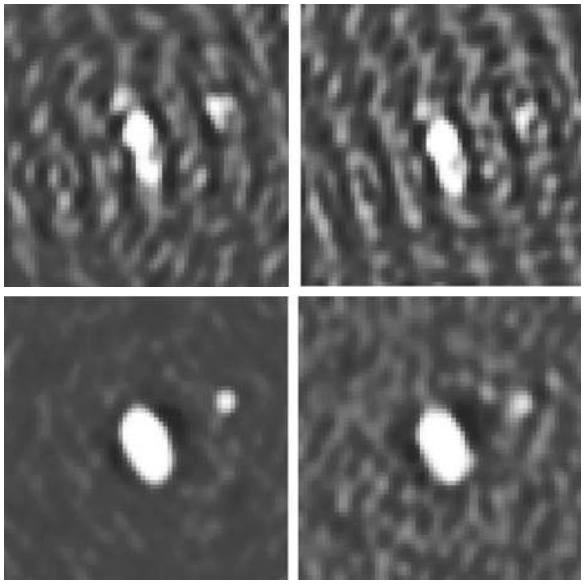

Fig. 1. Image reconstructions from simulated high-SNR data of an elliptical star with a companion which is approximately 3.4 magnitudes fainter than the primary. The upper images are reconstructed from simulated data using the beams from only 4 telescopes (i.e. 6 instantaneous baselines), while the lower images are reconstructed from an array of 6 telescopes (i.e. 15 instantaneous baselines). In each case an Earth-rotation synthesis of 6 hours duration was simulated. The leftmost images are reconstructed from uncorrupted phase data, simulating data from a phase-referenced system, while the rightmost images are reconstructed from closure-phase data. All images have the same greyscale levels. It can be seen that the difference between images reconstructed from 4-telescope data and those reconstructed from 6-telescope data is far greater than the difference between images constructed from phase-referenced data and from closure phase data.

information available, especially for larger numbers of telescopes, leaving the (u, v) coverage as the limiting factor in image quality. It is clear that given a choice between phase-referencing on a limited number of baselines and closure phases on a larger number of baselines, that the latter is to be preferred.

A less obvious requirement implied by a science emphasis on imaging is that of fringe tracking. Implicit in an imaging as opposed to astrometric observation is the assumption that the science targets will likely be resolved many times over by the longest baseline in the array. A necessary consequence of resolving the target is that the fringe contrast is low on the longest baselines. Low fringe contrasts mean low signal-to-noise ratios for fringe tracking (the SNR scales as the square of the fringe visibility) which means that fringe tracking on the longest baselines is the weak link in the imaging process. The most general way around this problem is the use of baseline bootstrap-

ping. This involves tracking fringes on a "chain" of short baselines (nearest-neighbour telescopes) and using this to infer the fringe motion on the longest baselines. Thus a general-purpose imaging interferometer must incorporate a bootstrapping fringe tracker. Furthermore, this fringe tracker should operate using group-delay tracking methods, since phase tracking methods are susceptible to short timescale fringe SNR "drop-outs" (due to, for example, AO system Strehl fluctuations). The likelihood of a drop-out somewhere along the chain of telescopes involved in bootstrapping grows with the length of the chain, rendering group-delay tracking, which is much more resistant to such drop-outs, the most competitive technique.

To summarise therefore, the optimum imaging instrument allows the combination of the beams from a large number of telescopes, allows the measurement of closure phase information, and incorporates a bootstrapping group-delay fringe tracker. This is the concept presented here.

3 BOBCAT concept description

A high-level block diagram of the proposed instrument, assuming a full complement of 6 input beams, is shown in Figure 2. If an initial implementation using only 4 input beams were desired, the fast switchyard identified at the top of the figure would not need to be installed, but could be introduced later as a potential upgrade.

3.1 Waveband selection and switchyard

Up to six path-compensated beams will enter the instrument from the VLTI delay lines. The beams them immediately enter a fast switchyard incorporating dichroic mirrors, which has two functions:

- It reflects light in the chosen science band (one of J, H or K bands) from a subset of four of the entering beams into the four input ports of the science combiner.
- It serves to transmit either the H or K-band light from all of the input beams to the fringe tracking combiner.

The switchyard is designed to be reconfigurable in less than 10 seconds, and will allow at least one permutation of every combination of four beams from up to six input beams to be selected, i.e. all baselines and closure triangles will be accessible to the science combiner. By using three configurations of the switchyard, all 15 baselines available from 6 telescope beams (or 12 of 15 baselines with two configurations) will be measurable within one or two minutes.

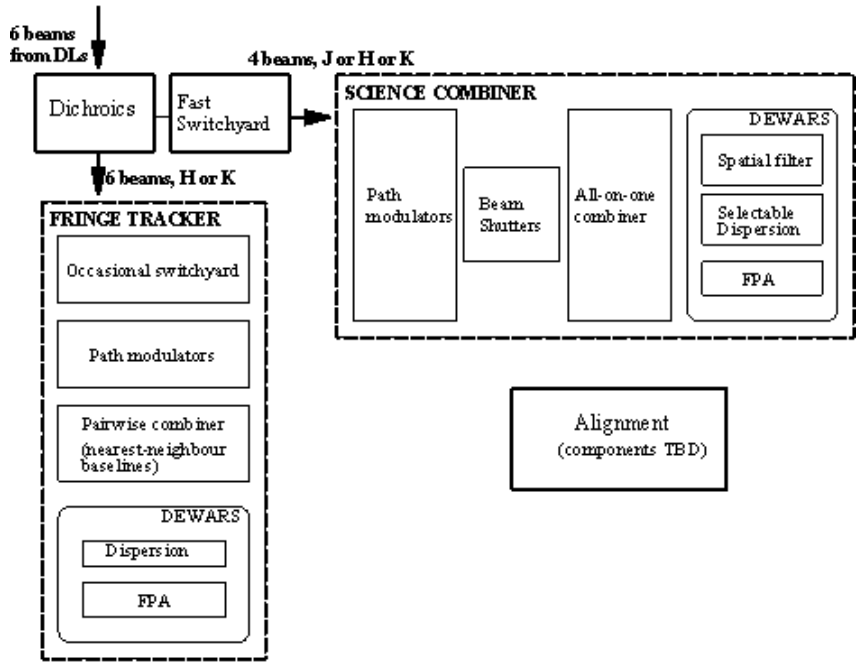

Fig. 2. Block diagram of the BOBCAT instrument concept assuming a maximum complement of six input beams. Light enters at the top, and is spectrally split between the science beam combiner at the right and the group-delay fringe tracking beam combiner to the bottom.

3.2 Internal group-delay fringe tracker

The fringe tracker will consist of a pairwise pupil-plane beam combiner that continuously measures fringes on the five (or equivalent for shorter chains) nearest-neighbour baselines in a bootstrapping "chain" of telescopes. This will most likely be implemented with the optical components mounted on discrete commercial or custom mounts. Low-noise hybrid FPA detectors will be used, such as those supplied by Rockwell or Raytheon, although only a small number ($<$100) of pixels will be used on any given device.

The fringe tracker will operate as a group-delay fringe tracker in either the H or K photometric band, with one of the two remaining bands from the set of J, H, and K being fed into the science combiner. The fringe tracker will be designed to maximize the raw signal-to-noise of the fringe measurement, as the data will not normally be used for science analysis. A small number (5) of spectral channels will be used. As the combiner will only serve to maintain the fringes within their coherence envelope, the OPD modulation of the input beams (provided internal to the instrument) will be relatively slow, and multiple short-exposure realisations of the fringes will be averaged to obtain each OPD estimate.

For a 6-beam instrument a total of 5 detector arrays will be required, each located in a separate dewar cooled to LN_2 temperatures and including a cold stop and a fixed dispersing element. This number may be revised downwards if further detailed studies suggest that more than two of the fringe-tracking outputs can be delivered to each focal-plane array or if fewer input beams are to be handled.

Within the group-delay tracker itself, there will be a separate additional switchyard to manage reconfigurations of the telescopes that feed the instrument. This will be adjusted when the VLTI array configuration is altered such that the short fringe-tracking baselines correspond to different pairings of the input beams as delivered to the instrument entrance port.

3.3 Science combiner

Our proposed implementation for the science beam combiner is a four-way pupil plane combiner. This will receive four input beams, and each of its four outputs will encode the full set of six fringe patterns appropriate to the four input beams. The choice of which input beams are fed to the science combiner will be determined by the instrument's "fast" switchyard which will allow rapid reconfiguration of the input beams.

Currently, we envisage using a high-stability optically-contacted beam combiner. A prototype combiner of this type has already been fabricated and tested in Cambridge (see Figure 3) and its behaviour and performance is well understood. Temporal modulation of the input beams so as to visualise the interference fringes will be provided by a separate set of PZT stacks actuating the mirrors feeding the combiner optics.

Each of the four combined beams will be fed to a cooled low-noise hybrid FPA via a spatial filter and a dispersing element. We expect the instrument will offer a choice of at least two, and possibly three, spectral resolution modes: low ($R \sim 30$), medium ($R \sim 300$) and high (R to be determined depending on science case and reference mission).

In this type of beam combiner, each of the four outputs provides interference signals on all six instantaneously-available baselines and so one detector and dewar interrogating a single output is sufficient to measure all the visibilities and closure phases. This type of design thus offers considerable flexibility in how the detectors and dewars are deployed; for example fewer than four detectors might be installed initially to reduce costs. Alternatively, detectors with fixed dispersion could be employed, with different spectral resolutions being provided at the different combiner outputs.

From a systems engineering approach, the choice of a four-way combiner rather than a six-way system has been based on a number of trade studies and serves to optimise the instantaneous fringe signal-to-noise ratio, to minimize risks associated with opto-mechanical stability, to minimize cross-talk between the different fringe signals, to simplify the optical design of the beam

combiner and to take maximum advantage of tried-and-tested components and methodologies.

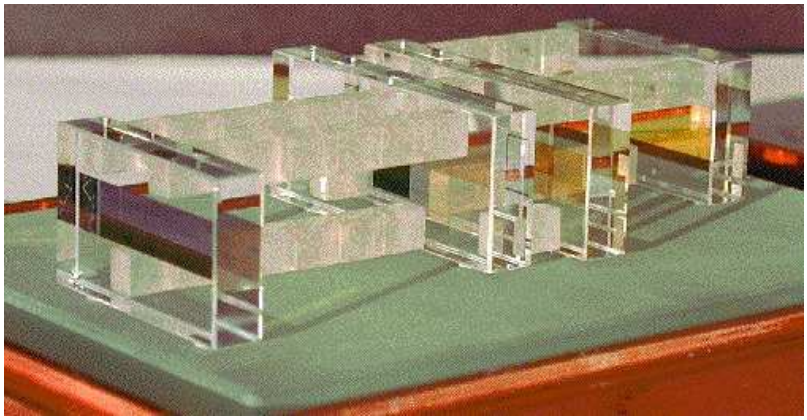

Fig. 3. Photograph of a prototype optically-contacted near-infrared four-way beam combiner for COAST. Once fabricated, this combiner requires no internal alignment. The overall footprint of this device, which has four inputs and four outputs, is 20cm x 10cm. A similar device for the VLTI would be expanded in scale.

4 Performance

4.1 Imaging capabilities

The proposed instrument will permit imaging by phase closure. The choice of a 6-beam instrument allows the desired (u, v)-plane coverage to be obtained with the minimum observing time (given that only six delay lines are available). Science data is recorded on 6 baselines and 4 closure triangles (3 independent) simultaneously, and the fast switchyard allows all 15 baselines and 10 independent closure phases available from 6 telescopes to be selected in a few minutes. For the same (u, v)-plane coverage, combining more beams together secures a greater fraction of the phase information: for example, the 6-beam concept preserves $2/3$ of the phase information, compared with $1/3$ for a 3-beam instrument such as AMBER.

One key feature of our proposed instrument is the ability to take advantage of baseline and, in most cases, wavelength bootstrapping by using a separate optimized fringe-tracking beam combiner. This will crucially allow science measurements to be made on the very longest VLTI baselines by monitoring the atmospheric fluctuations on the much shorter nearest-neighbor baselines between closely spaced telescopes. Unless a bright point

source reference is available within the isoplanatic patch, this will be the only way of measuring fringe amplitudes and phases for the resolved sources that will be the targets of many imaging studies.

4.2 Spectral coverage and resolution

The proposed instrument will be designed to record science data in any one of the *J, H* or *K* near-infrared photometric bands. In parallel, either the *H* or *K* photometric band will be used for fringe tracking. At each of the science beam combiner outputs at least two different spectral dispersions will be available: a low resolution mode with R$\sim$30, and an intermediate resolution mode with R$\sim$300. If there is a suitably compelling science case, then a high resolution mode will be considered as part of the conceptual design, although in the absence of such a science case we have not yet chosen an appropriate spectral resolution.

4.3 Limiting magnitude

The limiting magnitude for our proposed instrument will be determined by the limiting sensitivity of the group-delay fringe tracking sub-system. If a target is bright enough for the fringe tracker to operate, then arbitrarily long integration times (perhaps spread over multiple nights, at the same sidereal time) can be used to build up signal-to-noise in the science combiner. We have computed the fringe tracker limiting magnitude for several modes of operation, assuming the atmospheric parameters appropriate for "average" and "excellent" seeing conditions circulated to all work-package teams (see Table 1).

Table 1. Seeing parameters used for limiting magnitude and SNR calculations

Parameter (at λ = 500 nm)	Seeing FWHM /arcsec	Fried Parameter r_0 /cm	Coherence Time t_0/ms
"Average" seeing	0.8	12.6	6
"Best" seeing	0.5	20.2	15

We have assumed a basic integration of time of $2t_0$, and sky backgrounds of 14.4 mag/arsec^2 and 13.0 mag/arsec^2 in the H and K bands respectively, with the transmitted background from an Airy-disk sized area of sky being split between two combiner outputs. Spatial and temporal wavefront decorrelations due to the VLTI infrastructure have been included as described in the VLTI Interface Control Document, VLT-ICD-ESO-15000-1826, Issue 3.0 (henceforth "ICD"). These have been augmented with additional throughput losses, and spatial and temporal coherence loss factors for the instrument and assumed exposure time, as listed in Table 2. The thermal background

from the VLTI optical train was calculated assuming an emissivity of $(1-\eta)$, where η is the overall throughput. Finally, for ease of comparison, we have assumed a point source target.

Table 2. Instrument parameters used in performance calculations.

	Fringe Tracking combiner	**Science Combiner**
Instrument throughput (including detector QE)	40%	20%
Spatial wavefront error	$\lambda/20$ RMS @ 633nm	$\lambda/20$ RMS @ 633nm
Temporal phase jitter over coherent integration	$\lambda/20$ RMS @ 633nm	$\lambda/20$ RMS @ 633nm
Detector read noise	$3.0e^-$	$1.5e^-$
Visibility loss factor due to $2t_0$ integration	0.79	0.79

Detailed simulations of the group-delay tracking process were used to determinine the limiting photon flux required for group delay tracking in different observing conditions. In the process of deriving our limiting magnitudes quoted here, we have used a limiting flux values of twice those calculated from simulations in order to allow some margin of safety. For simplicity, values are given here for only two cases, a baseline between two UT's and a baseline between two AT's. In the UT case, we have assumed that the science target is also the reference star for the Adaptive Optics system. In order to calculate the Strehl delivered by the AO, we have assumed that the star has the colours of a G5 dwarf (V-H = 1.3 and V-K = 1.5). The ICD Strehl predictions as a function of guide star V magnitude for 0.65" seeing were used for both the "best" and "average" seeing cases.

Figures for the limiting sensitivity of the fringe-tracking subsystem for a number of the different observing modes are tabulated in Table 3 for average and best seeing conditions.

Table 3. Limiting sensitivities for the group-delay fringe tracking subsystem of the instrument.

	UT-UT (self-ref. AO)		**AT-AT**	
	H	***K***	***H***	***K***
"Average" seeing	13.5	14.4	12.7	12.7
"Best" seeing	13.6	14.5	13.9	13.5

It can be seen that the limiting sensitivities are adequate for the observation of many 10s of the brightest AGN, and hundreds of YSOs and other science targets.

4.4 Signal-to-noise ratio

In order to demonstrate the astronomical capability of the proposed instrument, we have also computed the signal-to-noise ratio for visibility amplitude estimation with the science beam combiner. With the type of combiner we are proposing, each of the four beam combiner outputs will deliver an independent estimate of the fringe signal. In the interest of clarity we have ignored the possibility of averaging the signals from multiple outputs (which could improve the SNR by a factor of between 2 and 4), and present below the signal-to-noise expected per single spectral channel and per single beam combiner output for various observing modes.

In deriving the values in Table 4, we have assumed an on-source incoherent integration time of 100 seconds, and have computed the signal-to-noise ratio expected for sources at three magnitudes (assuming Vega-type colours): one at the approximate sensitivity of the fringe tracker and also for 2 and 4 magnitudes brighter than this.

Table 4. Signal-to-noise ratios in 100s per spectral channel per beam combiner output for the science beam combiner, configured with a spectral resolution, R∼30. Values are given for a baseline between two UTs, and for a baseline between two ATs.

	UT-UT (self ref. AO)						**AT-AT**					
	J		**H**		**K**		**J**		**H**		**K**	
	mag	**SNR**	mag	**SNR**	mag	**SNR**	mag	**SNR**	mag	**SNR**	mag	**SNR**
"Average"	13	**0.03**	13	**1.5**	13	**10.5**	13	**0.01**	13	**0.13**	13	**0.54**
seeing	11	**1**	11	**18**	11	**53**	11	**0.5**	11	**3.3**	11	**11**
	9	**10**	9	**71**	9	**157**	9	**6**	9	**20**	9	**45**
"Best"	13	**0.05**	13	**2.4**	13	**13**	13	**0.3**	13	**1.3**	13	**3.2**
seeing	11	**1.6**	11	**21**	11	**55**	11	**4.3**	11	**14**	11	**22**
	9	**13**	9	**73**	9	**158**	9	**19**	9	**43**	9	**63**

It can be seen from the table that, for the faintest sources under average seeing conditions, the instrument will be limited by the signal-to-noise in the science beam combiner, and not by failure of the fringe-tracking sub-system. It should be noted that several techniques may be used to improve the science signal-to-noise ratio for faint targets, which have not been included in the above calculations, including coherent or incoherent combination of signals from multiple beam combiner outputs, incoherent combination of signals from adjacent spectral channels, the use of measurements from the fringe tracker to phase up consecutive basic integrations and hence extend the effective coherence time in the science combiner, and the use of a bright AO reference star for the UTs (where available).

4.5 Dynamic range

The dynamic range of images reconstructed from the visibility amplitude and closure phase measurements will depend on the number of data points and their random and systematic errors. The dynamic range expected in a map derived from n visibility data can in general be described by the following approximate formula:

$$\text{DynamicRange} = \frac{\sqrt{n}}{\sqrt{\left(\frac{\delta A}{A}\right)^2 + \delta\phi^2}}$$

where δA and $\delta\phi$ refer to the visibility amplitude and phase errors respectively.

Assuming that a sequence of calibrated measurements of the 15 baselines (and associated closure phases) associated with a 6-element subset of the UTs and ATs can be secured in 30 minutes, and that observations take place between Hour Angles of ± 3 hours, a suitable value for n will be of order 180. If we further assume fractional amplitude errors and phase errors of, say, 5%, this gives a dynamic range of approximately 200:1, i.e. 6 magnitudes. Hence, we can expect features at least 5 magnitudes fainter than the brightest unresolved component in the image to be detected reliably in any interferometric map.

5 Conclusions

We have presented a beam combiner concept which has been designed to exploit the wide range of interferometric science that is available from using the VLTI for model-independent imaging. A balanced approach has been taken to providing *all* the instrumentation needed to perform useful imaging science observations, including a multi-way bootstrapping fringe tracker. Proven high-efficiency bulk optics technologies have been used throughout in order to allow the observation of faint targets. A key feature of the design is that it can make use of the four ATs and six delay lines of the VLTI to their maximum advantage, for bootstrapping fringe tracking and rapid (u, v) coverage. Thus, even if scientific arguments are put aside, there is a strong case for a multi-beam correlator for the VLTI purely on the basis of maximising the return on the existing investment in the infrastructure at Paranal.

6 Acknowledgements

The authors would like to thank W. Warre and C. Coates for enhancing the depth of their understanding of the concept of complexity.